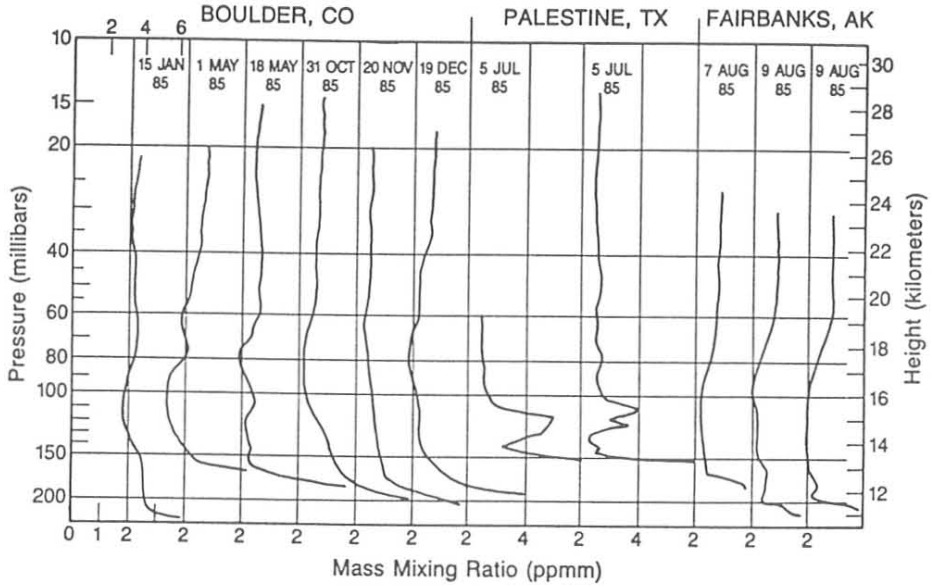

Figure 9.--Profiles of stratospheric water vapor mass mixing ratio (ppm) for 1985 at Boulder, CO; Palestine, TX; and Fairbanks, AK. Numbers along the top of the plot for the first water vapor profile are volume mixing ratios in ppm.

HALOCARBONS AND NITROUS OXIDE

Two new people were employed in 1985: A group leader, with specific expertise in calibration gas preparation, dissolved gas measurements, and infrared spectroscopy, who will arrive in 1986; and a CIRES employee, who began work in May as operations manager for field measurements.

Air samples continued to be collected weekly at BRW, NWR, MLO, and SMO, and weekly in January, November, and December only at SPO. These samples were returned to Boulder where CCl_3F (halocarbon F-11), CCl_2F_2 (F-12), and N_2O concentrations were determined by an EC-GC.

Our calibration standards for F-11 and F-12 were tied to the OGC scale. N_2O calibration standards were made at GMCC in Boulder and based on diluting a precisely known mixture of N_2O in CO_2 into a CO_2- and N_2O-free air mixture, measuring the CO_2 concentration, and thereby yielding the N_2O concentration. Cylinder 3072, which has been used exclusively as the source of calibration gas for sample analyses since 1977 in Boulder, was replaced by cylinder 3088 on 20 September because of low pressure. The SPO gas chromatograph was operated twice a week, analyzing air for F-11, F-12, and N_2O concentrations. Calibration gas came from cylinder 3083. Calibration standards will be produced by gravimetric techniques in the future.

Work on the RITS Project began with the design of an automated gas chromatograph and data processing system to measure the in situ air concentrations of N_2O, F-12, F-11, CH_3CCl_3, and CCl_4 at the baseline stations. Hardware and software were subsequently purchased, modified, and

tested. Installation of the system will begin in 1986 at SMO, BRW, and MLO. The system consists of a Hewlett-Packard Model 5890 EC-GC, a Nelson Analytical interface box, an HP9816 computer with Thinkjet printer, and an HP9133 hard disk and floppy drive.

Selected N_2O, F-12, and F-11 data from BRW, NWR, MLO, SMO, and SPO are shown in figs. 10, 11, and 12 for the period 1977-1985. The data from September 1984 through February 1985 have been excluded from the record because of problems with the detector's response. Least-squares regressions using a quadratic model fit to the data are represented by the solid lines in the figures. Estimated growth rates and associated standard deviations are also shown.

N_2O data have been corrected to account for the influence of CO_2 on the gas chromatographic analyses of air when it co-elutes with N_2O. Increasing levels of CO_2 in the atmosphere have enhanced our EC-GC's response to N_2O by approximately 0.2 ppb per ppm of CO_2 over the CO_2 range of 315-355 ppm.

Yearly means and standard deviations for the three constituents at the five stations are shown in Table 7. Years where data are missing have means estimated by the regression equation at midyear. The N_2O data record shows no significant (95%) change in the average rate of increase (0.64 ppbv yr^{-1}) for the 9 years for any of the stations. The rate of increase at SMO is increasing more rapidly than at other GMCC stations. The F-12 data likewise increase at a constant rate. However, in the Southern Hemisphere, F-12 concentrations are increasing 9% faster than in the Northern Hemisphere. All the stations except SPO show a significantly (99% confidence level) decreased rate of F-11 growth. The rate of growth of F-11 at SPO is also decreasing, but the large scatter in the data make it less significant (83% confidence level). Southern Hemispheric F-11 concentrations are growing 5% faster than at Northern Hemisphere sites. This is probably due to inter-hemispheric exchange rates being higher than Northern Hemisphere source rates.

Table 7.--Mean annual concentrations* of N_2O and halocarbons F-11 and F-12

	1977	1978	1979	1980	1981	1982	1983	1984	1985
N_2O (ppbv)									
BRW	301.8	301.5±0.2	301.9±0.2	301.6±0.3	302.8±0.2	303.4±0.1	303.3±0.2	304.4	304.9
NWR	300.5	301.1±0.3	301.9±0.2	303.3±0.3	303.3±0.2	304.6±0.2	305.2±0.2	305.8	306.2
MLO	300.8	300.2±0.3	301.5±0.2	302.0±0.3	302.8±0.3	303.8±0.2	303.8±0.2	305.3	306.0
SMO	302.0	302.6±0.3	304.1±0.2	304.5±0.3	305.5±0.3	307.1±0.2	307.4±0.2	308.8	309.5
SPO	299.4	300.1	300.8	301.4	302.0	302.5	302.9	303.3	303.7
F-12 (pptv)									
BRW	263.7	281.1±1.5	295.3±0.9	310.8±1.2	329.9±1.5	345.2±1.0	360.2±1.2	375.5	390.7
NWR	263.3	284.7±2.6	295.5±1.0	306.0±1.0	322.1±1.1	339.6±1.0	357.1±1.1	369.4	384.5
MLO	261.9	278.4±1.1	293.1±1.4	305.9±1.2	324.8±1.4	336.4±0.8	350.6±1.3	367.0	381.7
SMO	239.3	259.6±0.8	273.8±0.6	286.6±0.7	308.0±1.1	325.3±0.6	343.8±1.2	358.0	374.3
SPO	230.3	250.1	269.1	287.2	304.6	321.3	337.1	352.1	366.4
F-11 (pptv)									
BRW	154.1	165.0±0.7	173.9±0.6	183.8±0.5	193.5±0.7	201.8±0.5	212.1±0.7	219.4	227.4
NWR	151.1	162.3±1.0	169.0±0.7	180.1±0.7	188.1±0.5	197.8±0.7	208.4±0.6	215.2	223.7
MLO	145.1	156.3±0.6	166.7±0.7	177.1±0.6	186.0±0.5	193.8±0.5	205.0±0.7	212.6	220.5
SMO	135.7	148.2±0.6	158.3±0.5	167.7±0.4	178.1±0.7	188.4±0.4	198.1±0.6	205.4	213.1
SPO	139.1	150.1	160.7	171.0	180.8	190.3	199.3	208.0	216.3

*Values without standard deviations were calculated at midyear from the least-squares quadratic regression fits to the data.

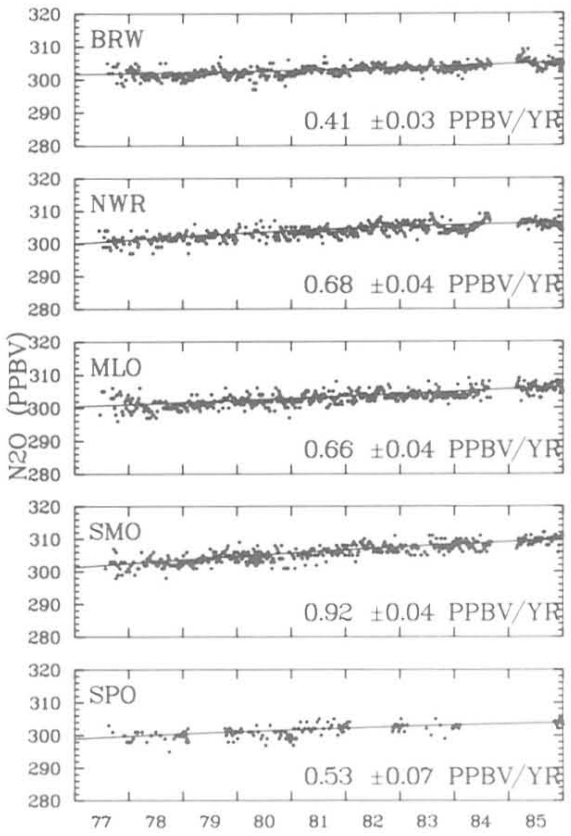

Figure 10.--Selected N_2O data record, and estimated growth rates and associated standard deviations.

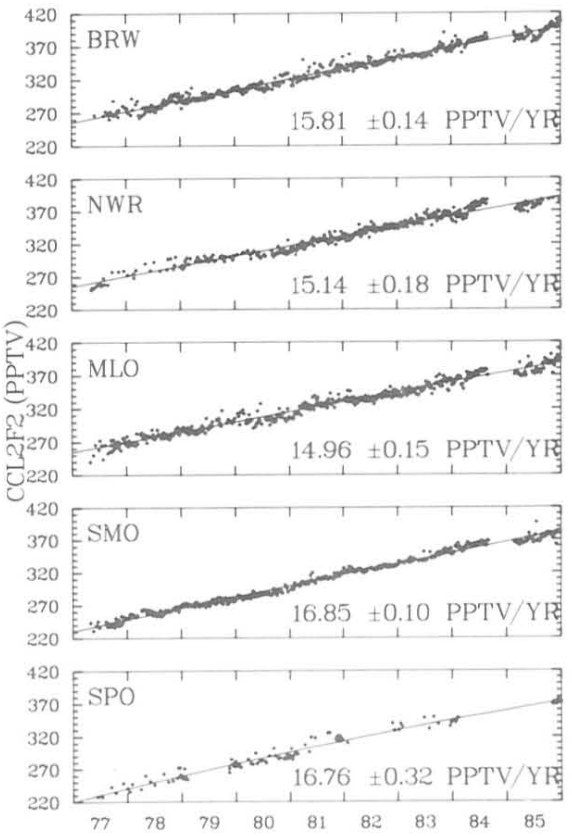

Figure 11.--Selected CCl_2F_2 (halocarbon F-12) data record, and estimated growth rates and associated standard deviations.

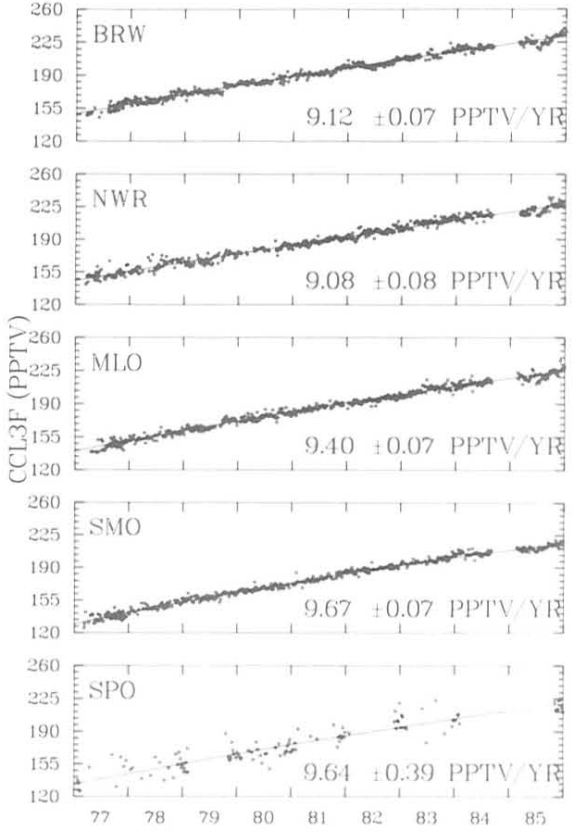

Figure 12.--Selected CCl_3F (halocarbon F-11) data record, and estimated growth rates and associated standard deviations.